Estimation of a Buried Pipe Location by Borehole Radar

Kazunori Takahashi
Graduate School of Environmental Studies
Tohoku University
Kawauchi 41, Sendai 980-8576, Japan
kazunori@cneas.tohoku.ac.jp

Motoyuki Sato
Center for Northeast Asian Studies
Tohoku University
Kawauchi 41, Sendai 980-8576, Japan
sato@cneas.tohoku.ac.jp

***Abstract*—A new parametric inversion technique to estimate a buried pipe location was developed for borehole radar cross-hole measurements. This technique evaluates the shapes of the approximated and measured arrival time curves instead of the first arrival time itself or wavefield in conventional inversion or tomographic techniques. In this study, we propose an algorithm of the technique and demonstrate its performance for synthetic and measured datasets.**

Keywords; ground penetrating radar (GPR); borehole radar; inversion

I. INTRODUCTION

To determine locations of buried pipes such as gas and water supplies, and subsurface cavities is important, for example before starting excavations. For borehole radar, the horizontal resolution is relatively poor and it is difficult to determine the horizontal location of pipes with high accuracy. Tomography and inversion techniques have generally been used for such investigations [1], [2]. Moreover, migration based imaging techniques also have been proposed [3]. However, these methods require densely sampled datasets and are computationally expensive. It is often difficult to acquire appropriate datasets for those techniques due to temporal and spatial limitations of the surveys especially in urban areas. In this contribution, we propose a new inversion scheme for bistatic transmission radar measurements.

Conventional radar tomography techniques try to image contrasts of electrical medium parameters. In other inversion techniques, e.g., [1] and [2], the total wavefield is modeled and compared to the measured wavefield. In contrast, the new inversion technique to be described here compares the shape of the first arrival time curves of measured data with that of theoretical curves. Furthermore, our inversion technique can use known information efficiently and explicitly. Unlike other inversion techniques, the result of this technique is not an image, but an explicit indication of the pipe location.

This paper describes the algorithm of the new inversion technique. Then it is applied to synthetic datasets and measured datasets to estimate a buried metallic pipe location. For the synthetic datasets by finite difference time domain (FDTD) method, the technique is demonstrated for a homogeneous and heterogeneous media to show the robustness of this technique against the inhomogeneity.

II. ALGORITHM OF THE INVERSION TECHNIQUE

A. Calculation of Approximated Arrival Times

Suppose that the target whose location we are trying to estimate is a metallic pipe with a known diameter buried in a homogeneous medium. Two vertical boreholes are located in the plane perpendicular to the pipe. Then approximately, the first arrivals are given by signals that propagate in this plane where the propagation paths are the shortest. The shapes of the first arrival time curves resulting from those paths are different for various locations of the pipe, transmitter, and receiver. If the pipe is located between the antennas, the signal cannot pass through the metallic pipe and propagates along the curved surface of the pipe as shown in Fig. 1, thus delaying the first arrival time. In this case the approximated first arrival time $t_{cal}(z, x, z_t, z_r)$ can be calculated using the ray-path model with a propagation velocity in the medium v, an assumed pipe location (z, x), and the approximated path length L for the transmitter at z_t and the receiver at z_r as follows.

$$t_{cal}(z, x, z_t, z_r) = L(z, x, z_t, z_r)/v \tag{1}$$

B. Evaluation of Curve Shapes

The approximated first arrival curves are compared with the arrival time curves from the measured datasets. Similarities of those curves are calculated for various assumed pipe locations, and a location that shows the highest similarity indicates the true location of the pipe. Picking first arrival times is difficult

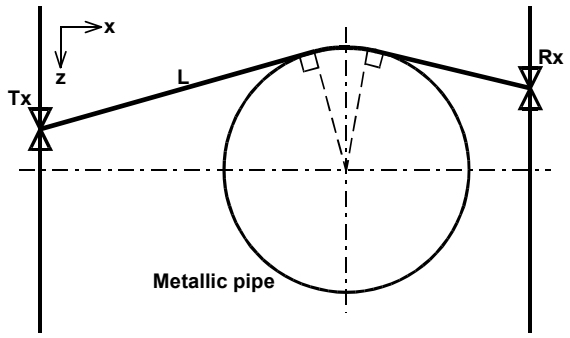

Figure 1. Model for calculation of the approximated first arrival time.

Report Documentation Page

Form Approved
OMB No. 0704-0188

1. REPORT DATE	2. REPORT TYPE	3. DATES COVERED
25 JUL 2005	**N/A**	**-**

4. TITLE AND SUBTITLE	5a. CONTRACT NUMBER
Estimation of a Buried Pipe Location by Borehole Radar	5b. GRANT NUMBER
	5c. PROGRAM ELEMENT NUMBER
6. AUTHOR(S)	5d. PROJECT NUMBER
	5e. TASK NUMBER
	5f. WORK UNIT NUMBER
7. PERFORMING ORGANIZATION NAME(S) AND ADDRESS(ES) **Graduate School of Environmental Studies Tohoku University Kawauchi 41, Sendai 980-8576, Japan**	8. PERFORMING ORGANIZATION REPORT NUMBER
9. SPONSORING/MONITORING AGENCY NAME(S) AND ADDRESS(ES)	10. SPONSOR/MONITOR'S ACRONYM(S)
	11. SPONSOR/MONITOR'S REPORT NUMBER(S)

12. DISTRIBUTION/AVAILABILITY STATEMENT
Approved for public release, distribution unlimited

13. SUPPLEMENTARY NOTES
See also ADM001850, 2005 IEEE International Geoscience and Remote Sensing Symposium Proceedings (25th) (IGARSS 2005) Held in Seoul, Korea on 25-29 July 2005. , The original document contains color images.

14. ABSTRACT

15. SUBJECT TERMS

16. SECURITY CLASSIFICATION OF:			17. LIMITATION OF ABSTRACT	18. NUMBER OF PAGES	19a. NAME OF RESPONSIBLE PERSON
a. REPORT **unclassified**	b. ABSTRACT **unclassified**	c. THIS PAGE **unclassified**	**UU**	**4**	

because of noise and limited frequency bandwidth. Generally, inversion techniques that use the first arrival times strongly depend on the quality of the pickings. Here we propose two schemes for evaluating the first arrival curve shapes that do not depend on the manual pickings.

1) Gradient Error Scheme: It is easy to pick the times $t_{meas}(z_t, z_r)$ at the maximum or a thresholded amplitude of each trace. The curves obtained in this way are no true first arrival time curves, but we assume them to be parallel to the true first arrival time curves. Then similarity in shape between the picked curve t_{meas} and the modeled curves t_{cal} can be evaluated by taking the error $e(z, x, z_t)$ of the gradients of t_{meas} and t_{cal}, which is given by integration along the receiver depth.

$$e(z,x,z_t) = \int dz_r \left| \partial_{z_r} t_{meas}(z_t, z_r) - \partial_{z_r} t_{cal}(z,x,z_t,z_r) \right| \quad (2)$$

This error can be calculated for each transmitter position. The total error for a series of transmitter positions is given by physical conjunction of the errors $e(z, x, z_t)$ and can be calculated by integration along the transmitter depth.

$$e_{total}(z,x) = \int dz_t \, e(z,x,z_t) \quad (3)$$

In this scheme, the lower error values indicate a higher similarity. Therefore, the minimum error value indicates a location that has the highest possibility of the true target location.

2) Correlation Scheme: From the modeled first arrival time curve, we firstly construct a binary reference $H(z, x, z_t, z_r, t)$. The reference is a matrix equal in size to the measured datasets. The elements of H that correspond to the approximated first arrival times are set to 1 and the others are set to 0. Cross-correlation between this reference and the measured dataset $S(z_t, z_r, t)$ indicates a similarity of the first arrival time curves, and the similarity is defined by the following expression.

$$R(z,x,z_t) = \max \left| \int\int d\tau dz_r \, S(z_t,z_r,\tau) H(z,x,z_t,z_r,t-\tau) \right| \quad (4)$$

To obtain the total correlation, such similarity values are to be integrated along the transmitter depth.

$$R_{total}(z,x) = \int dz_t \, R(z,x,z_t) \quad (5)$$

In this scheme, the higher correlation values indicate a higher similarity. Therefore, the maximum correlation value indicates a location that has the highest possibility of the true target location. Comparing gradient error scheme, the similarities can be evaluated without any picking operations by this scheme.

By using the two described schemes, we can avoid the error that occurs for picking the first arrival times from a measured dataset, and we do not need to consider how to define them. This makes our inversion scheme simple, robust and easy to operate.

III. Application to Synthetic Datasets

The inversion technique was applied to synthetic datasets generated by 3-D FDTD simulation of cross-hole fan measurements for the configuration shown in Fig. 2. The distance between two boreholes is 3.3 m, and a 1.0 m diameter metallic pipe is buried at a depth of 12.0 m and at a distance of 2.0 m from the transmitter borehole. The depth of the transmitter ranged from 11.0 m to 13.0 m with a 0.5 m step and of the receiver from 10.0 m to 14.0 m with a 0.1 m step.

A. Homogeneous Media Model

For a homogeneous media model, we set a permittivity of $20\varepsilon_0$ and a conductivity of 0.01 S/m to the whole surrounding media. Fig. 3 shows the gradient error maps for each transmitter depth. The total error map obtained by integration of all the error maps is shown in Fig. 4(a), and the total correlation obtained from all the correlation maps is shown in Fig. 4(b). In the error and correlation maps for a single transmitter position, the low error and the high correlation regions are not localized (see Fig. 3). In contrast, the total error and correlation maps have a localized region as shown in Figs. 4(a) and (b). The result from both evaluation schemes indicates a location that is exactly the same as the modeled location of the metallic pipe.

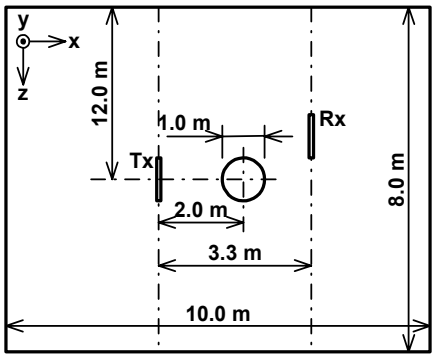

Figure 2. FDTD Model.

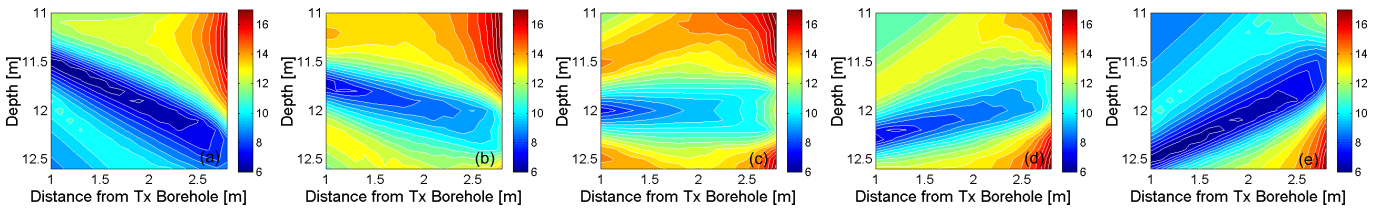

Figure 3. Gradient error maps for the trasmitter at depths of (a) 11.0 m, (b) 11.5 m, (c) 12.0 m, (d) 12.5 m, and (e) 13.0 m.

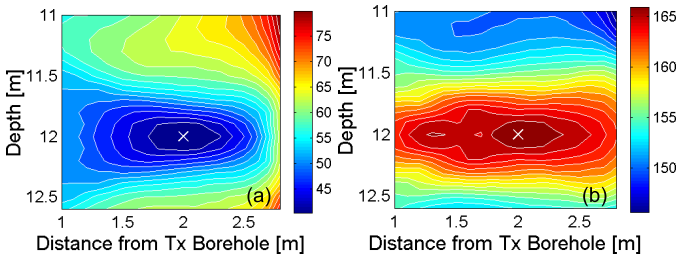

Figure 4. The results of the inversion technique calculated from synthetic datasets with homogeneous media model using (a) the gradient error scheme and (b) the correlation scheme. The crosses indicate the minimun value in (a) and the maximum value in (b).

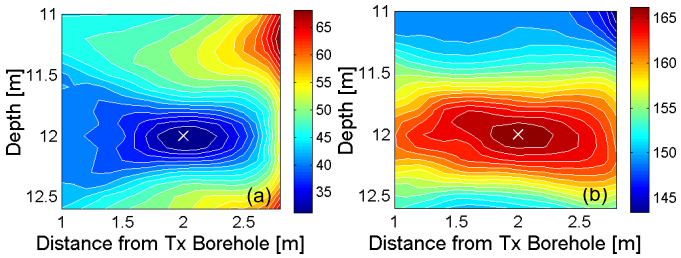

Figure 6. The results of the inversion technique calculated from synthetic datasets with heterogeneous media model using (a) the gradient error scheme and (b) the correlation scheme. The crosses indicate the minimun value in (a) and the maximum value in (b).

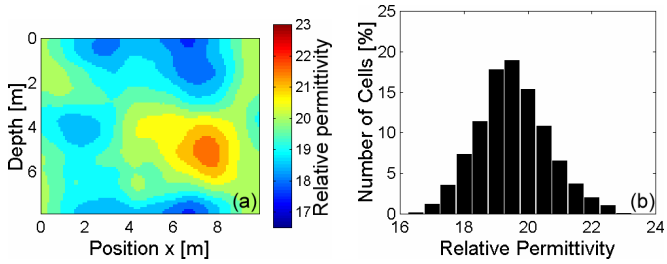

Figure 5. Relative permittivity distribution of the simulated heterogeneous media. (a) Vertical slice at y = 5.0 m. (b) Histogram of the simulated relative permittivity.

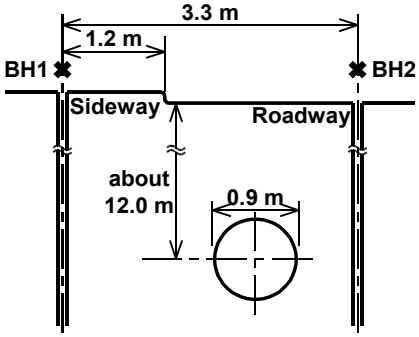

Figure 7. Geometrical sketch of the site.

B. Heterogeneous Media Model

For demonstrating a more realistic situation, a heterogeneous model was simulated in 3-D space employing a stochastic fractal model [4]. The simulated heterogeneous media model and its histogram are shown in Fig. 5. This model consists of 14 permittivities ranging from $16.5\varepsilon_0$ to $23.0\varepsilon_0$ and a constant conductivity of 0.01 S/m. This distribution has the mean permittivity of $19.5\varepsilon_0$ and the standard deviation of $1.1\varepsilon_0$. In the calculation of the inversion technique, we set the single permittivity of the medium to $20.0\varepsilon_0$ assuming homogeneous media. Fig. 6 shows the total error map and the total correlation map. Despite the localized regions are deformed comparing with the homogeneous model case shown in Fig. 4, they have the minimum error and the maximum correlation at the exact modeled location.

IV. Application to Measured Datasets

Field measurements were carried out in an urban area in Sendai, Japan, to determine the location of a metallic water pipe. The pipe is 0.9 m in diameter and the borehole separation is 3.3 m as shown in Fig. 7. In cross-hole fan measurements at this site, the transmitter was set in the borehole BH1 at depths of 11.0-13.0 m with a 0.5 m step, and the receiver was set in the borehole BH2 at 10.0-14.0 m with a 0.1 m step. An approximate depth of the pipe and the propagation velocity in the surrounding media were known from previous measurements. Fig. 8 shows the raw radar profiles acquired at each transmitter depth. In these data, the influence of geological discontinuities and inhomogeneity is visible, especially in Figs. 8(d) and (e). To prevent it from obscuring the inversion results, some of the traces are excluded. Wile the error and the correlation maps calculated for each transmitter position are not localized as in the case for the synthetic datasets, the total error and correlation maps have a localized region as shown in Figs. 9(a) and (b). The minimum error in the total error map is obtained at a depth of 12.1 m and at a distance of 2.1 m from the borehole BH1, and the maximum correlation in the total correlation map is obtained at a depth of 12.0 m and at the distance of 2.1 m from BH1. These results are consistent with known information from other measurements that the pipe is located at a depth of about 12.0 m and the borehole BH2 is closer to the pipe than BH1.

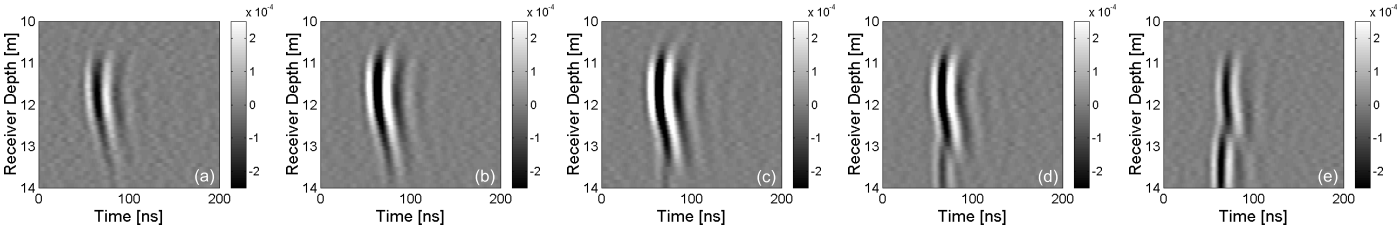

Figure 8. Radar profiles obtained by cross-hole fan measurements with the transmitter at (a) 11.0 m, (b) 11.5 m, (c) 12.0 m, (d) 12.5 m, and (e) 13.0 m depth.

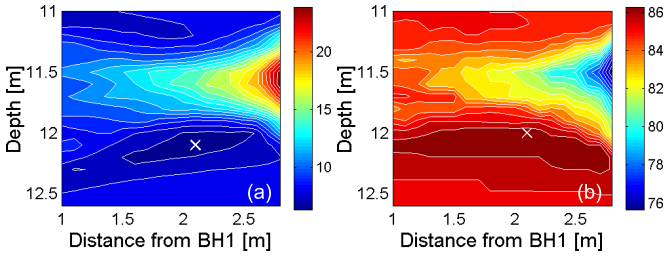

Figure 9. The results of the inversion technique for measured datasets using (a) the gradient error scheme and (b) the correlation scheme. The crosses indicate the minimum value in (a) and the maximum value in (b).

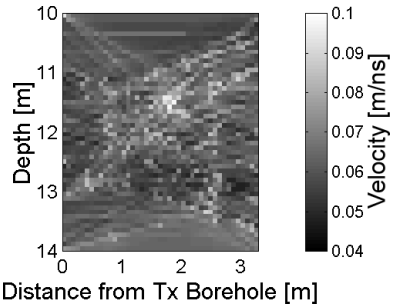

Figure 10. Velocity distribution obtained by travel time tomography.

V. DISCUSSION

By using the proposed two schemes to evaluate arrival time curve similarities, we could avoid the subjectivity of picking the true first arrival times. Moreover, we do not have to specify so many parameters. It needs to be specified where we pick times representing first arrival for the gradient error scheme, while for the correlation scheme, what kind of the reference used. Here the reason why the binary reference, which consists of only 0 and 1, was used is to reduce the parameters and consequently subjectivity.

This inversion technique works well to estimate a buried pipe location. However, for measured datasets, the estimated locations in the both of two total maps are not localized as clear as for the synthetic datasets. It is caused by the transmitter positions where the datasets were acquired. The maps for each transmitter depth are spreading along the lines connecting the transmitter positions and the center of the buried pipe as shown in Fig 3, and we cannot estimate the buried pipe location from those maps. Whereas the total maps can have localized region by taking a summation of all the maps, therefore, the datasets acquired by the transmitter at various position especially both above and bellow the pipe are necessary. In our case, the datasets acquired by the transmitter bellow the buried pipe cannot be used due to the strong effect of the geology as we can observe in Figs. 8(d) and (e). That is the reason why the maps spread. However, it could estimate the pipe location, although the datasets are few and sparse, and conversely, it might be possible to determine a buried location using only two datasets, which acquired at above and bellow the target.

A travel time tomography for these measured datasets could not image the pipe clearly as shown in Fig. 10, which is due to sparse sampling and the narrow measurement region. Therefore, this inversion technique is more suitable to determine a buried pipe location than tomographic technique for those conditions.

VI. CONCLUTION

The new inversion technique for estimation of a buried pipe location is proposed. For the synthetic datasets with homogeneous media, the inversion technique could retrieve the exact location of the buried metallic pipe using both the gradient error and correlation scheme, also for the datasets with the simulated heterogeneous media model. This indicates the inversion technique is rather robust against the inhomogeneity. Moreover, it could estimate the pipe location for the measured datasets in agreement with the known information. This shows that our technique works better than tomography for pipe location from sparse and small datasets. Further, it only requires rather simple calculations that can be done quickly. Therefore, this technique is robust, simple, stable, and easy to operate. It means it can easily be applied on-site, which is an enormous advantage for the practical use of this technique for underground surveying.

We think that our inversion technique can be applied to other targets, for instance tunnel-like cavities, with small modifications. Because the technique uses shape variations of the arrival time curves, and it can be applied to a target that delays or quickens the propagation time. Moreover, it can be applied to other bistatic radar transmission measurements such as vertical radar profiling (VRP) measurements by changing the geometry. Therefore, it has a high potential for application to various targets and measurements.

ACKNOWLEDGMENT

We acknowledge Dr. Hui Zhou from Nagasaki University, Japan for the processing of the travel time tomography and his suggestions, and Dr. Tadao Haryu from Hokko Georesearch, Japan for providing the opportunity to carry out the field experiment in Sendai, Japan. Part of this work was supported by JSPS Grant-in-Aid for Scientific Research (S)14102024.

REFERENCES

[1] H. Jia, T. Takenaka, and T. Tanaka, "Time-domain inverse scattering method for cross-hole radar imaging," *IEEE Trans. Geosci. Romote Sencing*, vol. 40, no. 7, pp. 1640-1647, July 2002.

[2] H-K. Choi, and J-W. Ra, "Detection and identification of a tunnel by iterative inversion from cross-borehole CW measurements," *Microwave Opt. Technol. Lett.*, vol. 21, no. 6, pp. 458-465, June 1999.

[3] H. Zhou, and M. Sato, "Subsurface cavity imaging by crosshole borehole radar measurements," *IEEE Trans. Geosci. Remote Sensing*, vol. 42, no. 2, pp. 335-341, Feb. 2004.

[4] B. Lampe, and K. Holliger, "Effects of fractal fluctuations in topographic relief, permittivity and conductivity on ground-penetrating radar antenna radiation," Geophisics, vol. 68, no. 6, Nov.-Dec. 2003.